Time-Dependent Density Functional Theory Study of the X-ray Absorption Spectroscopy of Acetylene, Ethylene, and Benzene on Si(100)

ARTICLE *in* THE JOURNAL OF PHYSICAL CHEMISTRY C · FEBRUARY 2007

Impact Factor: 4.77 · DOI: 10.1021/jp065160x

2 AUTHORS, INCLUDING:

Nicholas Besley
University of Nottingham
86 PUBLICATIONS **3,362** CITATIONS

Time-Dependent Density Functional Theory Study of the X-ray Absorption Spectroscopy of Acetylene, Ethylene, and Benzene on Si(100)

Nicholas A. Besley* and Adam Noble

School of Chemistry, University of Nottingham, University Park, Nottingham, NG7 2RD, UK

Received: August 10, 2006; In Final Form: January 12, 2007

The carbon 1s X-ray absorption spectroscopy (XAS) of acetylene, ethylene, and benzene in gas phase and adsorbed on the Si(100) surface is studied using time-dependent density functional theory (TDDFT) with hybrid exchange correlation functionals. The computed spectra are sensitive to the proportion of Hartree−Fock exchange in the exchange-correlation functional. The fraction of Hartree−Fock exchange is optimized to provide accurate predictions of the 1s → π^* excitation energies. In gas phase, the spectra of acetylene, ethylene and benzene are dominated by 1s → π^* excitations with further weaker bands at higher energies below the ionization threshold arising predominantly from Rydberg excitations. In the spectrum for ethane, bands arising from excitation to Rydberg and σ^*_{C-C} excitations are observed. For the molecules adsorbed on Si(100), excitations to Rydberg states are less evident. The calculations indicate that acetylene adsorbed on the Si(100) surface has an intense π^* band, which lies 1.5 eV lower than in gas phase, at an energy similar to gas-phase ethylene. Additional bands arising from σ^*_{Si-C} and σ^*_{C-H} excitations are observed also. The spectrum for ethylene on the surface has a broad feature that is largely due to the σ^*_{C-C} excitation, and at low energy a σ^*_{Si-C} band is predicted. Benzene is studied in two binding configurations. Both configurations have intense π^* bands arising from the 1s orbitals localized on the carbon atoms not bonded to the surface, and the location of this band is sensitive to the adsorption configuration. The results show that TDDFT with a modified hybrid exchange-correlation functional can provide accurate predictions of the XAS of organic molecules on the Si(100) surface and can assist in the elucidation of the structure of adsorbed molecules using polarized XAS.

Introduction

In recent years, X-ray absorption spectroscopy (XAS), often termed near edge X-ray absorption fine structure, has undergone tremendous advances due to the intensity and high-resolution obtainable with synchrotron radiation. These sources provide XAS with a richness in structure that can match more traditional UV spectroscopy. In addition, the local nature of core orbitals means that XAS provides an atom specific probe of electronic structure. Surface science is an area of research that has exploited XAS extensively, providing a probe of the electronic structure of adsorbed molecules yielding information on their structure and bonding.

The adsorption of organic molecules on the Si(100) surface has attracted considerable interest. Much of this work is motivated by the potential of organic molecules adsorbed on Si(100) to form a basis for a new generation of electronic device within existing microelectronics technology.[1] The Si(100) surface undergoes a characteristic (2 × 1) reconstruction in which adjacent atoms pair to form Si−Si dimers. These weak Si−Si dimers are reactive toward the adsorption of unsaturated hydrocarbons. Early high-resolution electron energy loss spectroscopic studies concluded that acetylene and ethylene adsorb on Si(100) forming sigma bonds with the weak Si−Si dimers. This is accompanied by a rehybridisation of the carbons with the silicon atoms of the dimer remaining bonded.[2−4] Theoretical studies also support this view of the bonding of acetylene and ethylene to Si(100).[5−6] The adsorption of benzene on the Si(100) surface has been the subject of a large number of studies. In a recent study, much of this earlier work was summarized and a comprehensive theoretical study reported.[7] The [4 + 2] configuration was found to be the structure at the global minimum.

Matsui and co-workers reported detailed studies of the carbon 1s XAS of acetylene and ethylene on the Si(100) surface.[8,9] For acetylene, resonances at 284.7, 286.0, 287.6, and 300 eV were identified and assigned to excitations to π^*_{C-C}, σ^*_{Si-C}, σ^*_{C-H}, and σ^*_{C-C} orbitals, respectively. Similarly, for ethylene resonances at 285.6, 287.0, 288.1, and 291.0 eV were assigned to σ^*_{Si-C}, π^*_{C-H2}, σ^*_{C-H2}, and σ^*_{C-C} orbitals. The σ^*_{C-C} resonances showed significant shifts from their gas-phase values. This was attributed to the sensitivity of the location of the σ^*_{C-C} resonance to the C−C bond length.[10] This was used to estimate the C−C bond lengths of the adsorbed species, which were found to be 1.36 Å for acetylene and 1.52 Å for ethylene.[8] There has been considerable debate regarding the validity of exploiting shape resonances to estimate bond lengths,[11−16] and a detailed discussion of this phenomena can be found elsewhere.[17]

Recently, fully polarized XAS studies of acetylene and ethylene on Si(100) have been reported.[18−19] These studies use a single domain Si(100) crystal and can probe the orientation of the adsorbed molecule with respect to the surface. Ethylene adsorbed on the surface showed a resonance at 291 eV; this was dominant with *x*-polarization but was also evident with *y*-polarization, where the C−C bond lies along the *x*-axis (see coordinates in Figure 1). This was assigned as the σ^* resonance and occurs at 10 eV lower than in gas-phase ethylene, which is consistent with the observation that the σ^* resonance shifts to

* Corresponding author. E-mail: nick.besley@nottingham.ac.uk.

10.1021/jp065160x CCC: $37.00
Published on Web 02/07/2007

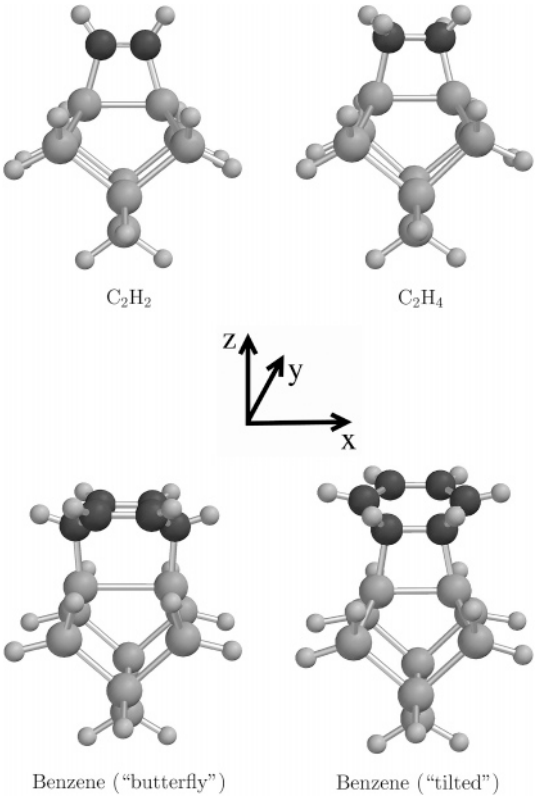

Figure 1. Acetylene, ethylene, and benzene adsorbed on the Si_9H_{12} cluster model of the Si(100) surface.

lower energies with increasing bond lengths.[10] The presence of the σ^* resonance in *x* and *y*-polarized spectra provides evidence for the C−C bond being rotated with respect to the Si−Si dimer of the surface. Additional resonances at 285.3 and 286.5 eV were assigned to σ^*_{Si-C} and σ^*_{C-H}, respectively. The σ^*_{Si-C} resonance appears weakly in the *y*-polarized spectra, which is consistent with the slight rotation of the C−C bond. The presence of the σ^*_{C-H} resonance in the *z*-polarized spectra indicates that the hydrogens are out of the plane of the C−C bond. For acetylene, a π^*_{C-C} resonance is observed at 283.8 eV. This resonance was observed in both parallel and perpendicular polarization spectra indicating the coexistence of two adsorption species. The σ^*_{Si-C} and σ^*_{C-H} resonances were found at 286.7 and 288.4 eV, respectively. The σ^*_{Si-C} resonance occurs 1.4 eV lower than ethylene, and a resonance at 299 eV was attributed to the σ^*_{C-C} excitation.

The carbon 1s absorption spectrum of benzene has been measured and shown to be rich in structure.[20−22] The carbon 1s → π^* excitation occurs at 285.1 eV. The absorption band lies between 284.5 and 286.5 eV and vibrational structure has been resolved and assigned. At higher energies below ionization, further discrete resonances are observed at approximately 287.2 and 288 eV and assigned to 3s and 3p Rydberg resonances, respectively.[22] These resonances are significantly weaker than the 1s → π^* band with the 3s resonance more intense than the 3p resonance. Additional resonances have been assigned to 4s and 4p Rydberg resonances and further π^* states. Substituted benzene rings show additional characteristic π^* excitations at higher energy.[23] The carbon 1s → π^* excitation has been studied in benzene clusters and shown to be red-shifted depending on the cluster size.[24] Kong et al. reported XAS spectra of benzene on Si(100).[25] The π^* excitation was found at 285 eV. Weaker bands at 287.7 and 289.5 eV were assigned to σ^*_{C-H} and σ^*_{Si-C} orbitals. The σ^*_{C-C} resonance was located at 292.2 eV. Polarized and angle resolved XAS also has been used to probe the structure of benzene adsorbed on Si(100).[26] The spectra are dominated by a band at 284.8 eV assigned to 1s → π^* excitations. This feature was evident in more than one polarization, indicating the adsorbed benzene is no longer flat. An additional weaker feature was observed at 286.9 eV. It was determined that benzene adopts the so-called "butterfly'' configuration corresponding to a 1-4-cyclohexadiene structure.

Experimental studies of XAS benefit greatly from theoretical calculations that can establish and quantify the relationship between the measured spectra and the underlying structural information. There are several approaches to the computation of XAS, and a wide variety of systems have been studied. Multiple scattering X_α methods can be applied to study XAS in both discrete and continuum regions.[27] Ab initio methods can also be applied to study XAS and much of this work has been reported by Pettersson, Nilsson, and co-workers (for example, see references 28−32). Within density functional theory, core excited states can be determined through variational optimization of the state within the constraint of single occupancy of the core orbital. This Kohn−Sham self-consistent field (ΔKS−SCF) approach includes all relaxation effects of the core hole and interaction of the excited-state with the molecular ion core. However, this method is not appropriate for spectral calculations due to the problem of optimizing higher excited states within separate Kohn−Sham calculations. The problem of optimizing individual states is avoided in the transition potential method.[33] In this approach, the ground and excited states are determined within a single calculation in which the core level has half an electron removed. This describes a balance between final and initial states.

An alternative approach is to use time-dependent density functional theory (TDDFT). TDDFT is well established as a method for studying valence excited states and computing electronic spectra.[34] Within the Tamm−Dancoff approximation (TDA)[35] of TDDFT, excitation energies and oscillator strengths are determined as the solutions to the eigenvalue equation

$$\mathbf{A}\mathrm{X} = \omega\mathbf{X} \tag{1}$$

The matrix **A** is given by

$$\mathbf{A}_{ai\sigma,bj\tau} = \delta_{ij}\delta_{ab}\delta_{\sigma\tau}(\epsilon_{a\sigma} - \epsilon_{i\tau}) + \mathbf{K}_{ai\sigma,bj\tau} \tag{2}$$

where **K** is the coupling matrix

$$\mathbf{K}_{ai\sigma,bj\tau} = (\psi^*_{a\sigma}(\mathbf{r})\psi_{i\sigma}(\mathrm{r})|\psi^*_{j\tau}(\mathbf{r}')\psi_{b\tau}(\mathbf{r}'))$$

$$+ \int \mathrm{d}\mathbf{r}\,\mathrm{d}\mathbf{r}'\,\psi^*_{a\sigma}(\mathbf{r})\psi_{i\sigma}(\mathbf{r})\frac{\delta^2 E_{\mathrm{XC}}}{\delta\rho_\sigma(\mathbf{r})\delta\rho_\tau(\mathbf{r}')}\psi^*_{j\tau}(\mathbf{r}')\psi_{b\tau}(\mathbf{r}') \tag{3}$$

The convention of *i*, *j*,... denoting occupied orbitals and *a*, *b*,... denoting virtual orbitals is adopted, while σ and τ are spin indices. **X** describes the linear response of the Kohn−Sham density matrix in the basis of the unperturbed molecular orbitals, ϵ_i are the orbital energies, ω are the excitation energies, and E_{XC} is the exchange correlation functional. Application of standard TDDFT methodology to the problem of the computation of XAS is problematic as these excitations comprise the highest lying excited states. Within TDDFT/TDA excitation energies are evaluated as the eigenvalues of the matrix **A**, eq 1. In most modern codes, the diagonalization of **A** is achieved through the iterative scheme of Davidson. This is efficient for valence states, but computation of core-excited states will require the full **A** matrix to be constructed and diagonalized. This results

in the computation of core excitation energies being computationally prohibitive. A solution to this problem is to perform the TDDFT calculation within the subspace of single excitations involving excitations from the relevant core orbital(s). One advantage of this approach is that it includes the coupling between the different singly excited configurations, and it has already been shown to work well for XAS by Stener and coworkers, who have applied it in the study a number of systems.[36−39] Our implementation is described in more detail elsewhere.[40] Within this scheme excitation energies can be computed within a reduced single excitation space. The following equation is solved

$$\bar{\mathbf{A}}\mathbf{X} = \omega\mathbf{X} \tag{4}$$

where

$$\bar{\mathbf{A}} = \mathbf{A}_{\bar{a}\bar{i}\sigma,\bar{b}\bar{j}\tau} \tag{5}$$

and $\{\bar{i}\}$ and $\{\bar{a}\}$ are subsets of occupied and virtual orbitals, respectively. For the study of molecules adsorbed on surfaces, it also can be beneficial to impose restriction within the virtual space. Virtual orbitals associated with the cluster do not provide an accurate representation of the extended surface and can lead to nonphysical bands in the computed spectrum. Furthermore, their removal also can reduce the computational cost of the calculations. Identification of these orbitals can be achieved through analysis of the molecular orbital coefficients of the virtual orbitals.[40] We recently used this methodology to study the excited states of CO on the Pt(111) surface[41] and the valence $\pi\pi^*$ excitations of a range of molecules adsorbed on the Si(100) surface.[42] The success of this approach depends on there being negligible coupling between the excitations of interest and those excluded from the single excitation space and is well suited to the study of XAS.

A number of studies have reported calculations of XAS (and X-ray emission spectroscopy) of atoms and molecules adsorbed on copper surfaces.[33,43−46] These include acetylene, ethylene, and benzene. These calculations adopt SCF, static exchange (STEX), and DFT transition potential methods and use cluster models of the surface. For acetylene and ethylene, the calculations find a reduction in the intensity of the π^* transition. In the case of acetylene, a pre-π^* shoulder is predicted. It has also been shown that resonances arising from excitations to Rydberg states are strongly quenched on adsorption.[47]

In this paper, TDDFT is used to study the polarized carbon 1s XAS of acetylene, ethylene, and benzene adsorbed on Si(100). We focus on discrete states below the ionization limit and use finite clusters to model the surface. The approach used here is not suitable for the study of the continuum states, although TDDFT can be extended to describe the electronic continuum.[48] However, the discrete virtual states are closely related to the continuum cross-section and can provide some insight into their nature. Polarized spectra are reported for gas-phase and adsorbed species, and the relationship between the spectral features and the molecular structure is investigated. All calculations use the Q-Chem software package,[49] except were indicated. All structures used in this study have been optimized at the B3LYP/6-31G* level of theory.

Effect of Exchange-Correlation Functional and Basis Set

Table 1 shows the computed carbon 1s → π^* excitation energies for acetylene, ethylene, and benzene with several exchange correlation functionals. The calculations include excitations from the 1s orbitals of all carbon atoms. The computed excitation energy is sensitive to the choice of functional. Pure Hartree−Fock exchange (CIS) predicts an excitation energy over 25 eV higher than the generalized gradient approximation (GGA) functionals BLYP[50,51] and EDF1.[52] As expected, the hybrid functionals, B3LYP[53,54] and B3PW91,[55] predict intermediate values that are closer to the GGA functionals. B3LYP gives a value of 275.9 eV, which is about 10 eV lower than the experimental value. Improving the quality of the functional through the addition of an asymptotic correction[56] has little effect on the 1s → π^* excitation energy as this affects primarily the Rydberg states. The B3LYP+CS00 functional[57] gives a value of 276.3 and 275.3 eV for acetylene and ethylene, respectively. This calculation with the B3LYP+CS00 functional was performed using the NWCHEM software package[58] and uses the full single excitation space. The value for benzene is not reported because of the size of the calculation. However, the introduction of the truncation introduces an error of less than 0.01 eV. This illustrates the validity of eq 4 for the calculation of XAS. The calculated oscillator strength is more sensitive to the truncation. Large errors in the 1s → π^* excitation energies obtained with the B3LYP functional have been observed previously.[59,60] It also was shown that core excitation energies calculated with a "half and half" functional with 50% Hartree−Fock exchange were in much better agreement with experiment. Table 1 shows 1s → π^* excitation energies computed with the half and half functional

$$\mathrm{BH^{0.50}LYP} = 0.50\mathrm{HF} + 0.42\mathrm{B} + 0.08\mathrm{S} + 0.81\mathrm{LYP} + 0.19\mathrm{VWN} \tag{6}$$

that is similar to the standard B3LYP functional

$$\mathrm{B3LYP} = 0.20\mathrm{HF} + 0.72\mathrm{B} + 0.08\mathrm{S} + 0.81\mathrm{LYP} + 0.19\mathrm{VWN} \tag{7}$$

where HF, B, and S are Hartree−Fock, Becke,[50] and Slater[60] exchange functionals, respectively, and LYP[51] and VWN[62] are correlation functionals. In agreement with previous work,[59] there is a significant improvement in accuracy. There is also an increase in the predicted oscillator strength. However, the excitation energies remain underestimated. Table 2 shows the sensitivity of the excitation energies computed with the $BH^{0.50}LYP$

TABLE 1: Variation of the Computed 1s → π^* Excitation Energy in eV with Exchange-Correlation Functional (6-31+G* Basis Set), Oscillator Strengths in Parentheses

method	C_2H_2	C_2H_4	C_6H_6
CIS	296.5 (0.17)	295.1 (0.18)	295.8 (0.56)
EDF1	270.3 (0.05)	269.4 (0.06)	270.1 (0.06)
BLYP	270.5 (0.04)	269.6 (0.05)	269.8 (0.07)
B3PW91	275.6 (0.07)	274.5 (0.08)	274.8 (0.22)
B3LYP	275.9 (0.07)	274.9 (0.08)	275.2 (0.22)
B3LYP+CS00	276.3 (0.08)	275.3 (0.08)	
$BH^{0.50}LYP$	283.9 (0.11)	282.8 (0.12)	283.7 (0.36)
exp[a]	285.8	284.3	285.2

[a] Values from experiment.[74]

TABLE 2: Variation of the Computed 1s → π^* Excitation Energy in eV with Basis Set ($BH^{0.50}LYP$ Exchange-Correlation Functional), Oscillator Strengths in Parentheses

basis set	C_2H_2	C_2H_4	C_6H_6
6-31+G*	283.9 (0.11)	282.8 (0.12)	283.7 (0.36)
6-31(3+,3+)G**	283.9 (0.11)	282.7 (0.12)	283.3 (0.35)
aug-cc-pVDZ	283.7 (0.11)	282.6 (0.12)	283.2 (0.35)
exp[a]	285.8	284.3	285.2

[a] Values from experiment.[74]

TABLE 3: Computed 1s → π* Excitation Energies (in eV) for a Test Set of Molecules

molecule	B3LYP	$BH^{0.50}LYP$	$BH^{0.57}LYP$	exp[a]
C_2H_2	275.9	283.9	285.7	285.8
C_2H_4	274.9	282.8	284.5	284.3
C_6H_6	275.2	283.3	285.1	285.2
*C*O	276.7	283.7	285.3	287.4
CH_2O	275.7	283.1	284.8	286.0
CHFO	278.2	285.4	287.0	288.2
CF_2O	280.7	287.8	289.5	290.9
C*O*	520.6	531.0	534.6	534.2
CH_2*O*	517.6	528.5	531.1	530.8
CHF*O*	518.5	529.6	532.2	532.1
CF_2*O*	519.2	530.5	533.1	532.7
CH*F*O	670.5	685.3	688.8	687.7
CF_2O	671.7	686.6	690.0	689.2
MAD[b]	12.3	2.5	0.7	

[a] Values from experiment.[74−76] [b]Mean absolute deviation.

functional to the basis set and indicates that there is little dependence on the basis set.

To improve the agreement with experiment further, the fraction of HF exchange in the hybrid exchange-correlation functional has been optimized to predict the experimental 1s → π* excitation energies of acetylene, ethylene, and benzene. This yielded the following functional

$$BH^{0.57}LYP = 0.57HF + 0.35B + 0.08S + 0.81LYP + 0.19VWN \quad (8)$$

Table 3 shows computed 1s → π* excitation energies for a range of molecules with the B3LYP, $BH^{0.50}LYP$, and $BH^{0.57}LYP$ functionals. The mean absolute deviation of the computed excitation energies from experiment is reduced from 12.3 eV for B3LYP to 2.5 eV for $BH^{0.50}LYP$ and to 0.72 eV by $BH^{0.57}LYP$. This demonstrates that although the functional has been optimized for acetylene, ethylene, and benzene, it does work well for a range of molecules.

While this functional is successful in predicting the 1s → π* excitation energies, it is likely to be less accurate for Rydberg states. This is because of the absence of an asymptotic correction, which is currently unavailable within our code. However, the increased proportion of HF exchange should improve the description of Rydberg states. Nakata et al. have developed also a functional, denoted CV-B3LYP, which is designed to describe core and valence excitations by varying the proportion of HF exchange in the functional. This functional has also been extended to describe Rydberg states.[60] In the methodology used here, there are no valence excitations, so there is no need for such a combined functional. The performance of the $BH^{0.57}LYP$ functional on the wider set of molecules is similar to the CV-B3LYP functional for basis sets of comparable quality to 6-31+G*. The accuracy of the CV-B3LYP functional with large basis sets approaches that of the unrestricted generalized transition state method.[63] The accuracy of the $BH^{0.57}LYP$ functional could be improved through the use of larger basis sets and a more detailed parametrization using a wider set of molecules. However, the functional in its current form provides a computational cheap and accurate platform for studying XAS that can be applied to chemisorbed molecules, and the $BH^{0.57}LYP$ functional with the 6-31+G* basis set was used in this study.

Gas Phase

Figure 2 shows the computed total and *x*, *y*, and *z*-polarized spectra for acetylene, ethylene, and ethane. For all spectra, the

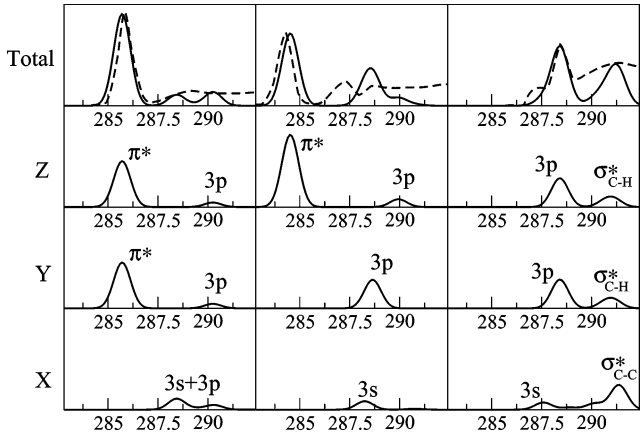

Figure 2. Computed total and *x*-, *y*-, and *z*-polarized spectra for acetylene (left column), ethylene (center), and ethane (right column). Broken line: experimental spectrum.[64]

C−C bond lies along the *x*-axis, and for ethylene the hydrogens lie in the *xy* plane. Spectra are generated by representing each computed electronic transition by a Gaussian function. It is necessary to choose a bandwidth for the Gaussians. For acetylene, ethylene, and ethane, a full width at half-maximum (fwhm) of 0.6 eV was used and for benzene a value of 0.4 eV was used. Also shown are experimental spectra adapted from ref 64. In this region of the spectrum, there is a large number of electronic excitations, however only a small number have significant intensity leading to the observed bands. In the current study, no attempt is made to model the broad continuum resonance observed at higher energy. Analysis of the transition dipole moments allow the theoretical spectrum to be decomposed into *x*, *y*, and *z*-polarized spectra. The assignment of the bands also is depicted in Figure 2.

The computed spectrum for acetylene is in good agreement with experiment. It is well known that the most intense band arises from excitation to the π^*_{C-C} orbital. The calculations are consistent with this and the π^*_{C-C} band is computed to lie at 285.7 eV. This band occurs in the *y* and *z*-polarized spectra. The core carbon 1s orbitals form symmetric ($1\sigma_g$) and antisymmetric ($1\sigma_u$) combinations. Analysis of the spectra shows the intense excitation to be a $1\sigma_u \rightarrow 1\pi_g^*$ transition. At higher energies, the calculations predict further bands at 288.4 and 290.2 eV arising from excitation to 3s and 3p Rydberg states. These bands also agree well with experiment. The polarized spectra show two types of Rydberg 3p excitation. The bands that appear in the *y*- and *z*-polarized spectra arise from excitation to 3p orbitals that lie perpendicular to the molecular axis and the band in the *x*-polarized spectrum to the 3p orbital parallel to the molecular axis. These can be denoted as $1\sigma_g \rightarrow 3p_\pi$ and $1\sigma_u \rightarrow 3p_\sigma$ excitations.

The computed spectrum for ethylene is qualitatively similar to acetylene. The spectrum is dominated by the π^*_{C-C} band at 284.5 eV. For ethylene, this band occurs only in the *z*-polarized spectra, and the resultant band is less intense. Like acetylene, this band corresponds to excitation from the $1\sigma_u$ orbital. The computed spectrum shows an intense band at approximately 288.6 eV arising predominantly from excitation to a 3p Rydberg state. On comparison with experiment, this band appears about 1.5 eV too high. Alternatively, the calculations may underestimate the intensity of the 3s band. A similar pattern was found in one particle Green's function calculations.[28] This error may be associated with the exchange-correlation functional, which has not be designed to describe Rydberg states. The TDDFT calculations compare well with genuine ab initio calculations.

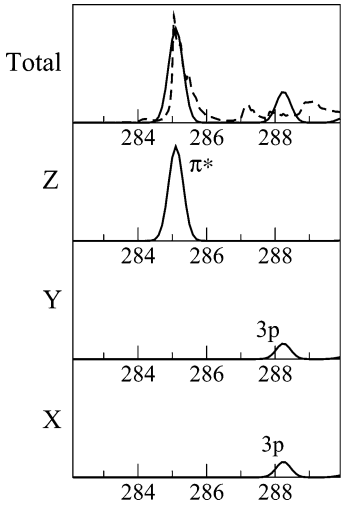

Figure 3. Computed total and *x*-, *y*-, and *z*-polarized spectra for benzene. Broken line: experimental spectrum.[22]

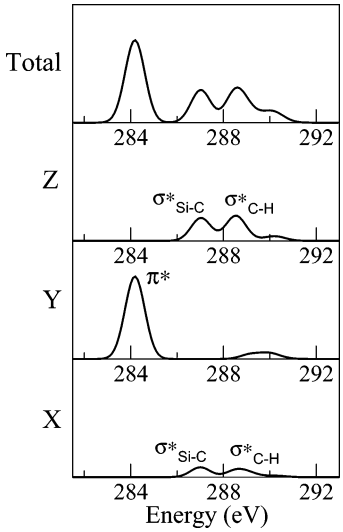

Figure 4. Computed total and *x*-, *y*-, and *z*-polarized spectra for acetylene adsorbed on Si(100).

In the open-shell electron attachment equations-of-motion coupled cluster calculations of Nooijen and Bartlett, the 1s → π^* excitation energies of acetylene and ethylene were predicted with an error of less than 0.2 eV,[65] while larger errors of up to 0.75 eV were reported in multireference configuration interaction calculations.[66] These methods do provide a more accurate description of the Rydberg states but cannot be used readily to study the molecules adsorbed on a surface.

The computed spectral profile for ethane is significantly different from those of the unsaturated hydrocarbons. The spectrum is no longer dominated by the π^*_{C-C} resonance, which is absent. The peaks at low energy arise from excitations to Rydberg states of s and p character. The assignments of these bands has been discussed in detail in the literature.[67−69] The small shoulder on the low-energy side of the band at 288.4 eV in experiment is not evident in the computed spectrum. However, this can assigned to the 3s Rydberg state. The band at 291.4 eV arises from σ^*_{C-H} and σ^*_{C-C} excitations. This band is considerably broader in experiment, since it lies close to the threshold ionization energy. For acetylene and ethylene, the σ^*_{C-C} excitations are predicted to lie in the continuum resonance at 301.7 and 296.1 eV, respectively. The trend in the computed σ^*_{C-C} excitation energies shows a significant decrease with increasing bond length, which is consistent with experiment,[10] although the σ^*_{C-C} excitation energies of acetylene and ethylene are significantly higher in experiment.

Figure 3 shows the computed and experimental[22] XAS spectrum for benzene. In the calculations, benzene lies in the *xy* plane. The XAS spectrum is dominated by the 1s → π^* band with weaker bands corresponding to Rydberg transitions evident at higher energy. The precise nature of these states has been the subject of some discussion.[20,70−72] The π^* band is computed to lie at 285.1 eV and appears in the *z*-polarized spectrum, which is consistent with benzene lying in the *xy* plane. In experiment, several distinct bands are evident at higher energy. The calculations predict significant intensity only for Rydberg 3p states. This discrepancy is similar to ethylene and may indicate deficiencies in the description of the Rydberg states.

Overall the calculations provide a good description of the experimental spectra. With the modified exchange-correlation functional, the computed 1s → π^* excitation energies are of comparable or superior accuracy than other theoretical approaches. Excitation energies for Rydberg states are less reliable, but these states are less important for the adsorbed species. For acetylene, ethylene, and benzene, intense π^* excitations are observed with weaker bands corresponding to Rydberg excitations lying at higher energies below the ionization limit. The ethane spectrum is different because there is no vacant π^* orbital, and low lying excitations correspond to Rydberg excitations. Bands arising from σ^*_{C-C} and σ^*_{C-H} excitations are observed. Consequently, the methodology provides a suitable framework to study the XAS of the adsorbed species.

Acetylene on Si(100)

In experiment, the XAS spectrum of acetylene on Si(100) shows three distinct bands below the resonance continuum. These bands are found at 283.8, 286.7, and 288.4 eV and have been assigned to π^*_{C-C}, σ^*_{Si-C}, and σ^*_{C-H} transitions, respectively.[19] The computed spectrum for acetylene adsorbed on the Si_9H_{12} model of the Si(100) surface is shown in Figure 4. For this cluster, the predicted C−C and Si−Si bond lengths are 1.36 Å and 2.37 Å, respectively. These are consistent with the experimental estimates of 1.32 − 1.37 Å and 2.44 ± 0.58 Å.[73] Excitations from both carbon 1s orbitals are included in the calculations. Spectra are generated with a fwhm of 0.4 eV. A number of bands are evident in the spectrum. The most intense band corresponds to the 1s → π^*_{C-C} excitation. The π^*_{C-C} band is predicted to lie at 284.2 eV, close to the experimental value of 283.8 eV.[19] This represents a red-shift of 1.5 eV from gas phase and lies close to the gas-phase value for ethylene of 284.5 eV. This red-shift is a consequence of the lengthening of the C−C bond on adsorption. This shift is a little smaller than the shift of 2 eV observed in experiment. In calculations of acetylene on the Cu(110) surface, the π^*_{C-C} band was computed to lie at 285 eV.[46] The π^*_{C-C} band occurs only in the *y*-polarized spectrum indicating that the C−C bond lies parallel to the silicon dimer axis.

Two bands at higher energy also are evident in the calculated spectrum. These are computed to lie at 287.0 and 288.4 eV and arise from σ^*_{Si-C} and σ^*_{C-H} excitations. The polarized spectra are consistent with these assignments. The σ^*_{C-Si} and σ^*_{C-H} bands are evident in *x*- and *z*-polarized spectra. The presence of the σ^*_{C-H} band in the *z*-polarized spectrum is a result of the hydrogens no longer lying along the C−C internuclear axis after adsorption. Excitations to Rydberg states are less prominent in the spectrum for adsorbed acetylene. This is consistent with

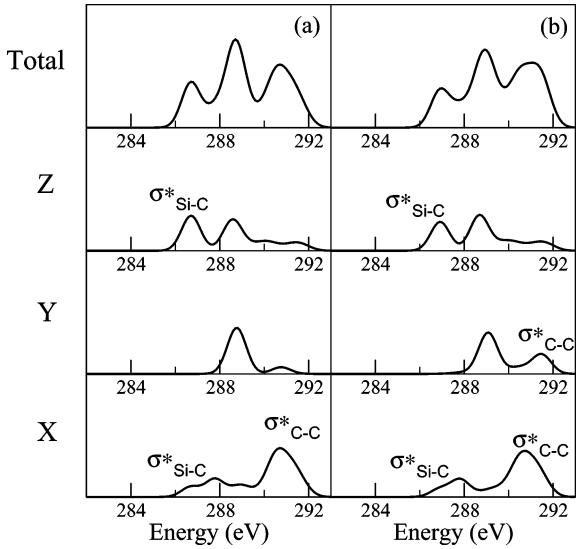

Figure 5. Computed total and *x*-, *y*-, and *z*-polarized spectra for ethylene adsorbed on Si(100). (a) C_{2V}; (b) C_2.

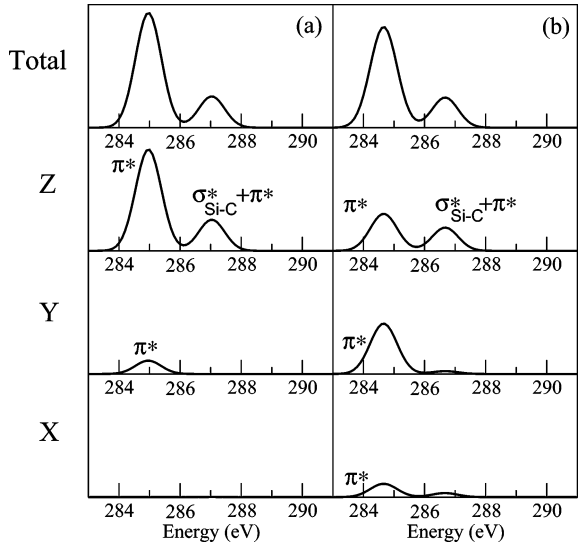

Figure 6. Computed total and *x*-, *y*-, and *z*-polarized spectra for benzene adsorbed on Si(100). (a) Butterfly; (b) tilted.

previous calculations that predict Rydberg states of *n*-octane to be quenched on adsorption.[47]

Ethylene on Si(100)

Once ethylene is adsorbed on the Si(100) surface, there is no longer a vacant π^* orbital and its spectrum has many of the characteristics of gas-phase ethane. The experimental spectrum of ethylene on Si(100) is dominated by a broad resonance at 291 eV, which is assigned to the σ^*_{C-C} excitation. At lower energies, resonances corresponding to σ^*_{Si-C} and σ^*_{C-H} are observed also at 285.3 and 286.5 eV, respectively.[18] Figure 5 shows the computed carbon 1s XAS spectrum of ethylene on the Si_9H_{12} cluster in two orientations. Excitations from the two carbon 1s orbitals are included. Including excitations to all virtual orbitals leads to appearance of large resonances that correspond to excitation to orbitals associated with the Si_9H_{12} cluster. These excitations are an artifact of the cluster surface model and do not correspond to excitations that would be observed in experiment. To remove these excitations, a virtual orbital is included in the reduced virtual space, $\{\bar{a}\}$, if the sum of the square of the normalized molecular orbital coefficients of the basis functions of the acetylene carbon and hydrogen atoms and the silicon atoms of the cluster bonded to acetylene is greater than 0.2. Spectra are represented using a fwhm of 0.6 eV.

In the first configuration, the C−C bond lies along the *x*-axis parallel to the surface dimer and has C_{2V} symmetry. The spectrum has three distinct bands at 286.7, 288.6, and 291.1 eV. Analysis of the molecular orbitals shows the low-energy band arises from excitation to the σ^*_{Si-C} orbital. This band is evident in *x*- and *z*-polarized spectra, which is consistent with this assignment. The computed excitation is higher than the value determined in experiment. This feature is computed to lie at a similar energy to the corresponding excitation for acetylene. Experiment predicts the σ^*_{Si-C} excitation to be lower in energy for ethylene. The broad feature at 291 eV has contributions from several transitions. The largest component occurs at 291.1 eV and corresponds to the σ^*_{C-C} excitation. This excitation only occurs in the *x*-polarized spectrum; this is a result of the constraint of C_{2V} symmetry. A small feature in the *y*-polarized spectrum is evident at this energy, but this arises from a different transition. The predicted excitation energy is close to the value of 291 eV from experiment. The σ^*_{C-C} excitation energy is predicted to be 291.4 eV for gas-phase ethane. The C−C bond length of the adsorbed ethylene is 0.04 Å longer than gas-phase ethylene. The shift in the σ^*_{C-C} excitation energy is consistent with the observed strong dependence of σ^*_{C-C} excitation energy with C−C bond length.[10] Other contributions to this band arise from a mixture of excitations, including excitation to orbitals largely localized on the cluster and also to ethylene Rydberg orbitals.

Experiment shows the C−C bond of ethylene to be twisted with respect to the Si−Si dimer axis.[18] The cluster models used in this work provide an approximate description of the extended surface. Structural effects that arise from the extended nature of the surface, including adsorbate−adsorbate interactions, will not be captured using such models. To model the true experimental structure more closely, a second configuration in which the C−C bond is twisted with respect to the surface dimers is considered. This is the fully optimized structure and has a dihedral angle between the two carbon atoms and the two silicon atoms at the top of the cluster of 9.5°. The shape of the computed spectrum is similar to the C_{2V} configuration. The location of the σ^*_{C-Si} band is similar to the more symmetric configuration at 286.9 eV. The broad feature at 291 eV has a significant contribution from the σ^*_{C-C} excitation. However, for the twisted C_2 configuration this feature is clearly evident in the *y*-polarized spectrum.

Benzene on Si(100)

The computed spectra for benzene on the Si_9H_{12} cluster in butterfly and tilted bonding configurations are shown in Figure 6. Both spectra show an intense peak arising from 1s → π^* excitations with a smaller peak at about 2 eV higher in energy, which is consistent with experiment.[26] The π^* bands arise from excitation from the 1s orbitals associated with the carbons not bonded to the surface. For the butterfly configuration, the π^* band is clearly evident in *z*- and *y*-polarized spectra and for the titled configuration it is evident in all polarized spectra; this reflects the low symmetry of the adsorbed benzene molecule in the tilted configuration. The predicted 1s → π^* excitation energies are 285.0 and 284.5 eV for the butterfly and tilted configurations, respectively. This suggests the location of the π^* band is sensitive to the adsorption geometry. Experiment

predicts a value of 284.8 eV for the butterfly configuration. The theoretical results are very close to the experimental value. It is worth noting that the predicted value for the butterfly configuration is closer to experiment. However, reliable predictions at this level of precision are probably beyond the current methodology. The smaller band at higher energy has been assigned to the σ^*_{C-H} transition.[25] In our calculations, this band appears predominantly in the *z*-polarized spectrum, which is inconsistent with this assignment. The calculations show this band to arise from excitation from the 1s orbitals of the carbon atoms bonded to the surface to a mixture of the σ^*_{Si-C} and π^* orbitals.

Conclusions

A TDDFT formalism has been applied to study the polarized carbon 1s XAS of some prototypical hydrocarbons in gas phase and adsorbed on the Si(100) surface in the region of the spectrum below the ionization threshold. With standard functionals, such as B3LYP, the computed excitation energies are much lower than experiment. However, increasing the amount of HF exchange in the functional leads to a much better agreement with experiment. In this work, we have used a hybrid functional that has been optimized to give accurate 1s $\rightarrow \pi^*$ excitation energies. The surface has been modeled using a small cluster model. This surface model should capture the dominant effects, although some effects of an extended surface model, such as adsorbate−adsorbate interactions will be neglected. However, the methodology used here could be extended to study larger extended surface models.

In gas phase, the spectra of acetylene, ethylene, and benzene are dominated by intense 1s $\rightarrow \pi^*$ bands with weaker bands at higher energies arising from excitation to Rydberg states. The spectrum for ethane shows bands arising from Rydberg states at low energies with a more intense band arising from σ^*_{C-H} and σ^*_{C-C} excitations. The computed spectra reproduce experiment well, in particular for valence excitations. For ethylene and benzene, larger discrepancies are found for the Rydberg bands. This is likely to be associated with the asymptotic form of the functional, which is not suited for this type of excitation.

The spectra for the adsorbed species are significantly different from the gas phase. This is largely associated with the change in hybridization of the carbons. The spectrum of acetylene on the surface has the characteristics of the gas-phase spectrum of ethylene, while the spectrum of ethylene on the surface resembles the gas-phase spectrum of ethane. The π^* excitation for acetylene on the surface is 1.3 eV lower than is gas phase, which is close to the value for ethylene in the gas phase. The Rydberg bands observed in the gas-phase spectra are less evident in the spectra for the adsorbed molecules. However, additional bands at lower energy corresponding to σ^*_{Si-C} excitation can be distinguished. Benzene adsorbed on the surface has intense π^* bands that arise from core orbitals localized on the carbons not bonded to the surface. The location of the π^* band is sensitive to the binding geometry. At higher energy lies a band that can be associated with excitation from the 1s orbitals of the carbon atoms bonded to the surface to a mixture of σ^*_{Si-C} and π^* orbitals. The calculations are consistent with recent experimental work and show that careful analysis of the polarized spectra can provide information on specific details of the bonding geometry. This shows that experimental XAS studies in conjunction with theory provides a useful structural probe.

Acknowledgment. N.A.B. is grateful to the Engineering and Physical Sciences Research Council for funding in particular for the award of an Advanced Research Fellowship (GR/R77636). NWChem Version 4.7, as developed and distributed by Pacific Northwest National Laboratory, P. O. Box 999, Richland, Washington 99352 USA and funded by the U.S. Department of Energy, was used to obtain some of these results. N.A.B. would like to thank the referees for their comments on the manuscript.

References and Notes

(1) Chen, J.; Reed, M. A.; Rawlett, A. M.; Tour, J. M. *Science* **1999**, *286*, 1550.
(2) Nishijima, M.; Yoshinobu, J.; Tsuda, H.; Onchi, M. *Surf. Sci.* **1987**, *192*, 383.
(3) Yoshinobu, J.; Tsuda, H.; Onchi, M.; Nishijima, M. *J. Chem. Phys.* **1987**, *87*, 7332.
(4) Huang, C.; Widdra, W.; Wang, X. S.; Weinberg, W. H. *J. Vac. Sci. Technol., A* **1993**, *11*, 2250.
(5) Silvestrelli, P. L.; Toigo, F.; Ancilotto, F. *J. Chem. Phys.* **2001**, *114*, 8539.
(6) Pan, W.; Zhu, T.; Yang, W. *J. Chem. Phys.* **1997**, *107*, 3981.
(7) Jung, Y.; Gordon, M. S. *J. Am. Chem. Soc.* **2005**, *127*, 3131.
(8) Matsui, F.; Yeom, H. W.; Imanishi, A.; Isawa, K.; Matsuda, I.; Ohta, T. *Surf. Sci. Lett.* **1998**, *401*, L413.
(9) Matsui, F.; Yeom, H. W.; Matsuda, I.; Ohta, T. *Phys. Rev. B* **2000**, *62*, 5036.
(10) Stöhr, J.; Sette, F.; Johnson, A. L. *Phys. Rev. Lett.* **1984**, *53*, 1684.
(11) Kempgens, B.; Köppe, H. M.; Kivimäki, A.; Neeb, M.; Maier, K.; Hergenhahn, U.; Bradshaw, A. M. *Phys. Rev. Lett.* **1997**, *79*, 35.
(12) Kempgens, B.; Kivimäki, A.; Köppe, H. M.; Neeb, M.; Bradshaw, A. M.; Feldhaus, J. *J. Chem. Phys.* **1997**, *107*, 4219.
(13) Sorensen, S. L.; Wiklund, M.; Sundin, S.; Ausmees, A.; Kikas, A.; Svensson, S. *Phys. Rev. B* **1998**, *58*, 1879.
(14) Haack, N.; Ceballos, G.; Wende, H.; Baberschke, K.; Arvanitis, D.; Ankudinov, A. L.; Rehr, J. J. *Phys. Rev. Lett.* **2000**, *84*, 614.
(15) Arvanitis, D.; Haack, N.; Ceballos, G.; Wende, H.; Baberschke, K.; Ankudinov, A. L.; Rehr, J. J. *J. Electron Spectrosc. Relat. Phenom.* **2000**, *113*, 57.
(16) Farren, R. E.; Sheehy, J. A.; Langhoff, P. W. *Chem. Phys. Lett.* **1991**, *177*, 307.
(17) Piancastelli, P. N. *J. Electron Spectrosc. Relat. Phenom.* **1999**, *100*, 167.
(18) Hennies, F.; Föhlisch, A.; Wurth, W.; Witkowski, N.; Nagasono, M.; Piancastelli, M. N. *Surf. Sci.* **2003**, *529*, 144.
(19) Pietzsch, A.; Hennies, F.; Föhlisch, A.; Wurth, W.; Nagasono, M.; Witkowski, N.; Piancastelli, M. N. *Surf. Sci.* **2004**, *562*, 65.
(20) Schwarz, W. H. E.; Chang, T. C.; Seeger, U.; Hwang, K. H. *Chem. Phys.* **1987**, *117*, 73.
(21) Ma, Y.; Sette, F.; Meigs, G.; Modesti, S.; Chen, C. T. *Phys. Rev. Lett.* **1989**, *63*, 2044.
(22) Rennie, E. E.; Kempgens, B.; Köppe, H. M.; Hergenhahn, U.; Feldhaus, J.; Itchkawitz, B. S.; Kilcoyne, A. L. D.; Kivimäki, A.; Maier, K.; Piancastelli, M. N.; Polcik, M.; Rüdel, A.; Bradshaw, A. M. *J. Chem. Phys.* **2000**, *113*, 7362.
(23) Cooney, R. R.; Urquhart, S. G. *J. Phys. Chem. B* **2004**, *108*, 18185.
(24) Bradeanu, I. L.; Flesch, R.; Kosugi, N.; Pavlychev, A. A.; Rühl, E. *Phys. Chem. Chem. Phys.* **2006**, *8*, 1906.
(25) Kong, M. J.; Teplyakov, A. V.; Lyubovitsky, J. G.; Bent, S. F. *Surf. Sci.* **1998**, *411*, 286.
(26) Witkowski, N.; Hennies, F.; Pietzsch, A.; Mattsson, S.; Föhlisch, A.; Wurth, W.; Nagasono, M.; Piancastelli, M. N. *Phys. Rev. B* **2003**, *68*, 115408.
(27) Sheehy, J. A.; Gil, T. J.; Winstead, C. L.; Farren, R. E.; Langhoff, P. W. *J. Chem. Phys.* **1989**, *91*, 1796.
(28) Liegener, C.; Ågren, H. *Phys. Rev. B* **1993**, *48*, 789.
(29) Nyberg, M.; Luo, Y.; Triguero, L.; Pettersson, L. G. M.; Ågren, H. *Phys. Rev. B* **1999**, *60*, 7956.
(30) Ostrom, H.; Fohlisch, A.; Nyberg, M.; Heske, C.; Pettersson, L. G. M.; Nilsson, A. *Surf. Sci.* **2004**, *559*, 85.
(31) Cavalleri, M.; Odelius, M.; Nilsson, A.; Pettersson, L. G. M. *J. Chem. Phys.* **2004**, *121*, 10065.
(32) Cavalleri, M.; Odelius, M.; Nordlund, D.; Nilsson, A.; Pettersson, L. G. M. *Phys. Chem. Chem. Phys.* **2005**, *7*, 2854.
(33) Triguero, L.; Pettersson, L. G. M.; Ågren, H. *Phys. Rev. B* **1998**, *58*, 8097.
(34) Tozer, D. J.; Amos, R. D.; Handy, N. C.; Roos, B. O.; Serrano-Andres, L. *Mol. Phys.* **1999**, *97*, 859.
(35) Hirata, S.; Head-Gordon, M. *Chem. Phys. Lett.* **1999**, *314*, 291.
(36) Stener, M.; Fronzoni, G.; de Simone, M. *Chem. Phys. Lett.* **2003**, *373*, 115.

(37) Fronzoni, G.; Stener, M.; Reduce, A.; Decleva, P. *J. Phys. Chem. A* **2004**, *108*, 8467.
(38) Fronzoni, G.; De Francesco, R.; Stener, M. *J. Phys. Chem. B* **2005**, *109*, 10332.
(39) Fronzoni, G.; De Francesco, R.; Stener, M.; Causa, M. *J. Phys. Chem. B* **2006**, *110*, 9899.
(40) Besley, N. A. *Chem. Phys. Lett.* **2004**, *390*, 124.
(41) Besley, N. A. *J. Chem. Phys.* **2005**, *122*, 184706.
(42) Besley, N. A.; Blundy, A. J. *J. Phys. Chem. B* **2006**, *110*, 1701.
(43) Triguero, T.; Pettersson, L. G. M. *Surf. Sci.* **1998**, *398*, 70.
(44) Pettersson, L. G. M.; Ågren, H.; Luo, Y.; Triguero, L. *Surf. Sci.* **1998**, *408*, 1.
(45) Nyberg, M.; Odelius, M.; Nilsson, A.; Pettersson, L. G. M. *J. Chem. Phys.* **2003**, *119*, 12577.
(46) Öström, H.; Nordlund, D.; Ogasawara, H.; Weiss, K.; Triguero, T.; Pettersson, L. G. M.; Nilsson, A. *Surf. Sci.* **2004**, *565*, 206.
(47) Weiss, K.; Öström, H.; Triguero, T.; Ogasawara, H.; Garnier, M. G.; Pettersson, L. G. M.; Nilsson, A. *J. Electron Spectrosc. Relat. Phenom.* **2003**, *128*, 179.
(48) Zangwill, A.; Soven, P. *Phys. Rev. A* **1980**, *21*, 1561.
(49) Kong, J.; White, C. A.; Krylov, A. I.; Sherrill, C. D.; Adamson, R. D.; Furlani, T. R.; Lee, M. S.; Lee, A. M.; Gwaltney, S. R.; Adams, T. R.; Daschel, H.; Zhang, W.; Ochsenfeld, C.; Gilbert, A. T. B.; Kedziora, G.; Maurice, D. R.; Nair, N.; Shao, Y.; Besley, N. A.; Maslen, P. E.; Dombroski, J. P.; Baker, J.; Byrd, E. F. C.; Van Voorhis, T.; Oumi, M.; Hirata, S.; Hsu, C.-P.; Ishikawa, N.; Florian, J.; Warshel, A.; Johnson, B. G.; Gill, P. M. W.; Head-Gordon, M.; Pople, J. A. *J. Comput. Chem.* **2000**, *21*, 1532.
(50) Becke, A. D. *Phys. Rev. A* **1988**, *28*, 3098.
(51) Lee, C.; Yang, W.; Parr, R. G. *Phys. Rev. B* **1988**, *37*, 785.
(52) Adamson, A. D.; Gill, P. M. W.; Pople, J. A. *Chem. Phys. Lett.* **1998**, *284*, 6.
(53) Becke, A. D. *J. Chem. Phys.* **1993**, *98*, 1372.
(54) Stephens, P. J.; Devlin, F. J.; Chabalowski, C. F.; Frisch, M. J. *J. Chem. Phys.* **1994**, *98*, 11623.
(55) Becke, A. D. *J. Chem. Phys.* **1993**, *98*, 5648.
(56) Tozer, D. J.; Handy, N. C. *J. Chem. Phys.* **1998**, *109*, 10180.
(57) Casida, M. E.; Jamorski, C.; Casida, K. C.; Salahub, D. R. *J. Chem. Phys.* **1998**, *108*, 4439.
(58) Apr, E; Windus, T. L.; Straatsma, T. P.; Bylaska, E. J.; de Jong, W.; Hirata, S.; Valiev, M.; Hackler, M.; Pollack, L.; Kowalski, K.; Harrison, R.; Dupuis, M.; Smith, D. M. A.; Nieplocha, J.; Tipparaju, V.; Krishnan, M.; Auer, A. A.; Brown, E.; Cisneros, G.; Fann, G.; Früchtl, H.; Garza, J.; Hirao, K.; Kendall, R.; Nichols, J.; Tsemekhman, K.; Wolinski, K.; Anchell, J.; Bernholdt, D.; Borowski, P.; Clark, T.; Clerc, D.; Dachsel, H.; Deegan, M.; Dyall, K.; Elwood, D.; Glendening, E.; Gutowski, M.; Hess, A.; Jaffe, J.; Johnson, B.; Ju, J.; Kobayashi, R.; Kutteh, R.; Lin, Z.; Littlefield, R.; Long, X.; Meng, B.; Nakajima, T.; Niu, S.; Rosing, M.; Sandrone, G.; Stave, M.; Taylor, H.; Thomas, G.; van Lenthe, J.; Wong, A.; Zhang, Z. *NWChem, A Computational Chemistry Package for Parallel Computers*, Version 4.6; Pacific Northwest National Laboratory: Richland, WA, 2004.
(59) Nakata, A.; Imamura, Y.; Otsuka, T.; Nakai, H. *J. Chem. Phys.* **2006**, *124*, 094105.
(60) Nakata, A.; Imamura, Y.; Nakai, H. *J. Chem. Phys.* **2006**, *125*, 064109.
(61) Dirac, P. A. M. *Proc. Cambridge. Philos. Soc.* **1930**, *26*, 376.
(62) Vosko, S. H.; Wilk, L.; Nusair, M. *Can J. Phys.* **1980**, *58*, 1200.
(63) Hu, C.-H.; Chong, D. P. *Chem. Phys. Lett.* **1996**, *262*, 729.
(64) Hitchcock, A. P.; Brion, C. E. *J. Electron Spectrosc. Relat. Phenom.* **1977**, *10*, 317.
(65) Nooijen, M.; Bartlett, R. J. *J. Chem. Phys.* **1995**, *102*, 6735.
(66) Barth, A.; Buenker, R. J.; Peyerimhoff, S. D.; Butscher, W. *Chem. Phys.* **1980**, *46*, 149.
(67) Väterlein, P.; Fink, R.; Umbach, E.; Wurth, W. *J. Chem. Phys.* **1998**, *108*, 3313.
(68) Weiss, K.; Bagus, P. S.; Wöll, Ch. *J. Chem. Phys.* **1999**, *111*, 6834.
(69) Urquhart, S. G.; Gillies, R. *J. Phys. Chem. A* **2005**, *109*, 2151.
(70) Horsley, J. A.; Stöhr, Hitchcock, A. P.; Newbury, D. G.; Johnson. A. L.; Sette, F. *J. Chem. Phys.* **1985**, *83*, 6099.
(71) Yokoyama, T.; Seke, K.; Morisada, I.; Edamatsu, K.; Ohta, T. *Phys. Scr.* **1990**, *41*, 189.
(72) Ågren, H.; Vahtras, O.; Carravetta, V. *Chem. Phys.* **1995**, *196*, 47.
(73) Terborg, R.; Baumgärtel, P.; Lindsay, R.; Schaff, O.; Giessel, T.; Hoeft, J. T.; Polcik, M.; Toomes, R. L.; Kulkarni, S.; Bradshaw, A. M.; Woodruff, D. P. *Phys. Rev. B* **2000**, *61*, 16697.
(74) Francis, J. T.; Knkvist, C.; Lunell, S.; Hitchcock, A. P. *Can. J. Phys.* **1994**, *72*, 879.
(75) Francis, J. T.; Kosugi, N.; Hitchcock, A. P. *J. Chem. Phys.* **1994**, *101*, 10429.
(76) Robin, M. B.; Ishii, I.; McLaren, R.; Hitchcock, A. *J. Electron Spectrosc. Relat. Phenom.* **1988**, *47*, 53.